

1 **From messy chemistry to ecology: autocatalysis and heritability in prebiotically plausible**
2 **chemical systems**

3 Tymofii Sokolskyi^{1,2}, Bruno Cuevas Zuviria³, Sydney Gargulak¹, Esau Allen¹, David Baum^{1,2}

4 1 - Wisconsin Institute for Discovery, University of Wisconsin-Madison, Madison, WI 53715, USA

5 2 - Department of Botany, University of Wisconsin-Madison, Madison, WI 53706, USA

6 3 - Centro de Biotecnología y Genómica de Plantas, Universidad Politécnica de Madrid (UPM) -

7 Consejo Superior de Investigaciones Científicas (CSIC-INIA), Pozuelo de Alarcón, Madrid, Spain

8 28223

9 **Abstract**

10 A key question in origins-of-life research, is whether heritability, and thus evolution,
11 could have preceded genes. Out-of-equilibrium chemical reaction networks with multiple
12 autocatalytic motifs may provide chemical “memory” and serve as units of heritability, but
13 experimental validation is lacking. We established conditions that may be conducive to the
14 emergence of heritable variation and developed methods to search for heritability and
15 autocatalysis. We prepared a food set (FS) of three organic species, three inorganic salts and
16 pyrite. We conducted a serial dilution experiment where FS was incubated for 24 hours, after
17 which a 20% fraction was transferred into freshly prepared FS that went through the same
18 procedure, repeated for 10 generations. To serve as controls, we also incubated the fresh
19 solutions in each generation. We compared the chemical composition of transfer vials and no-
20 transfer controls using liquid chromatography-mass spectrometry (LCMS), with metrics adapted
21 from ecology and evolutionary biology. While variability was high, focusing on a subset of
22 chemicals with more consistent patterns revealed evidence of heritable variation among vials.
23 Using rule-based chemical reaction network inference, constrained by the LCMS data, we
24 identified a plausible FS-driven chemical reaction network that was found to contain numerous
25 autocatalytic cycles.

26

27

28 **Introduction**

29 The capacity for evolution is one of the key attributes of life (Joyce, 1994). As a result,
30 finding chemical systems that are capable of adaptive evolution, yet simple enough to emerge
31 spontaneously under prebiotic conditions is a central goal of origins-of-life research (Paul &
32 Joyce, 2004). A necessary prerequisite for adaptive evolution is a mechanism to generate
33 heritable variation. In modern evolutionary biology, heritability is due to the presence of
34 variation in self-replicating genetic molecules, which tends to result in a correlation between
35 the traits of parents and their progeny. However, theoretical work suggests that heritable
36 variation need not depend upon the existence of genetic molecules like RNA or DNA but can
37 also arise in chemical reaction networks (CRNs) that contain self-amplifying, which is to say
38 autocatalytic, motifs (Wächtershäuser 1988; Segre et al., 2001a; Vasas et al. 2012; Baum 2018).
39 However, to date, experimental data validating these claims are lacking.

40 It has been proposed that life emerged when CRNs driven out of equilibrium by a
41 continuing influx of “food” established some form of spatial structure, for example in micelles
42 (Segre et al., 2001a) or mineral surfaces (Wächtershäuser et al. 1988; Baum, 2018). Given
43 occasional seeding of new autocatalytic motifs by rare seeding events, different spatial
44 locations could establish different dynamical states that would tend to be passed on to other

45 locations via dispersal (Peng et al., 2022; Baum et al. 2023). However, such autocatalytically
46 “encoded” heritability has yet to be shown in the lab and, indeed, evidence of autocatalysis in
47 small-molecule organic chemistry remains scant (Orgel, 2008).

48 Since heritability depends on their being multiple autocatalytic motifs (Vasas et al.,
49 2015), a minimal requirement for a CRN to show evolvability is that it generates a diverse set of
50 chemical compounds. Such compositional diversity is readily achieved in prebiotic chemistry via
51 combinatorial explosions (Warr, 1997; Colon-Santos et al., 2019; Matange et al., 2023),
52 especially in the presence of heat and catalytic surfaces (de Graaf et al., 2023). It seems
53 theoretically possible, therefore, to initiate combinatorial explosions in the lab in such a way as
54 to foster sufficient autocatalytic complexity to result in the emergence of heritable variation.

55 Despite the desirability of creating laboratory conditions suitable for the emergence of
56 heritability and evolution, there remain many challenges. The simplest to solve is the
57 establishment of systems that can be interpreted as “parents” and “offspring” (Baum &
58 Vetsigian, 2017). This could be achieved using a set of continuously stirred tank reactors
59 (Happel & Stadler, 1999) or by establishing multiple parallel lineages in a recursive transfer
60 paradigm, also known as chemical ecosystem selection (Vincent et al., 2019).

61 Multiple parent-offspring lineages can be used to calculate an analog of narrow-sense
62 heritability, by looking at the slope of a linear regression of parent-offspring chemical
63 characteristics (Sokolskyi et al., 2024). Other options include an approach developed by
64 Guttenberg et al. (2015), which uses principal component analysis to estimate the number of
65 heritable states in a complex system, or a method proposed by Segrè et al. (2001b) based on
66 the threshold cosine similarity among vectors of chemical composition.

67 In this paper we used a chemical ecosystem selection paradigm in conditions where a
68 simple, small-molecule food solution yields a combinatorial explosion of chemical complexity.
69 Then, using the detailed chemical fingerprints generated by liquid-chromatography/mass-
70 spectrometry (LCMS), we evaluated evidence of heritability. We find that the vials receiving
71 transfers from prior generations tend to have more chemical diversity than no-transfer controls
72 and that, in many generations, the parent and offspring vials tend to be more chemically similar
73 to each other than to other vials. Finally, *in silico* chemistry analyses, guided by the LCMS data,
74 revealed evidence of autocatalytic processes that could plausibly explain heritability. Our
75 analysis not only provides the first direct (if weak) evidence of heritability but also suggests
76 promising avenues for further research into the *de novo* emergence of heritability and
77 evolutionary change.

78
79
80

Materials & Methods

Compound	Concentration	Vendor	Part number
Formic acid	10 mM	Aqua Solutions	F6088
Acetic acid	10 mM	Fischer Scientific	BP2401
Methanol	10 mM	Thermo Fischer Scientific	A4564
Ammonium hydroxide	4 mM	VWR	EM1.05432.1011
Sodium bicarbonate	20 mM	Sigma Aldrich	S6014

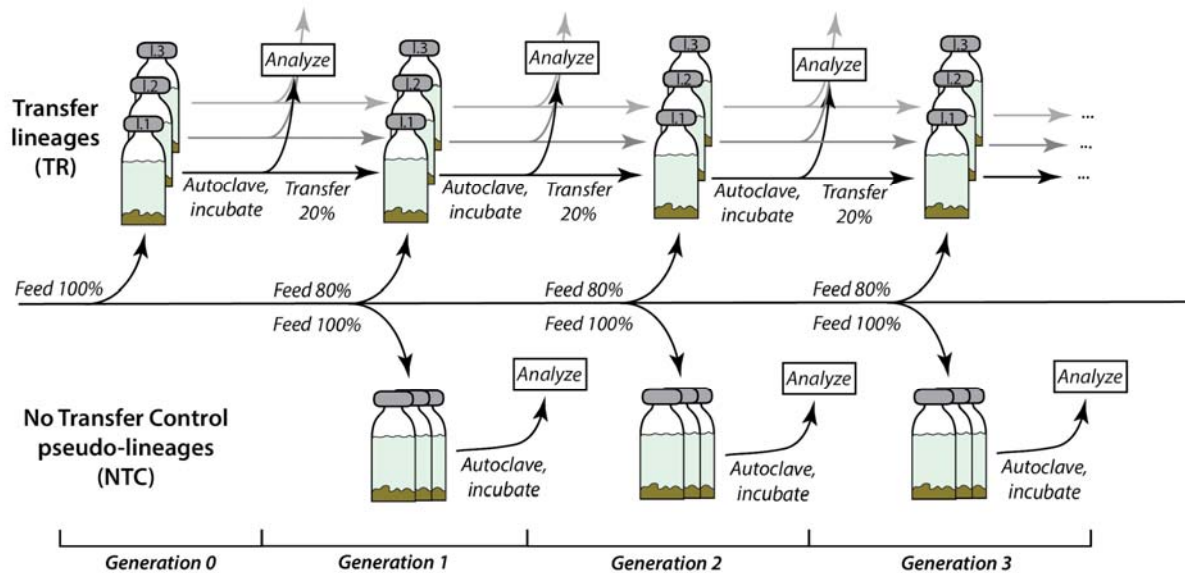
Sodium trimetaphosphate	0.1 mM	Sigma Aldrich	T5508
Pyrite	100 mg/mL	VWR	100198-728

81 **Table 1.** Composition of the food set (FS).

82

83 **Solution preparation.** We prepared a food set (FS) solution consisting of 6 compounds and a
84 mineral, pyrite (**Table 1**), which is known for its catalytic activity (de Graaf et al., 2023). All
85 components except pyrite were mixed in water and stored at 4°C until use. An aliquot of FS was
86 added to pyrite every generation of the experiment. The organic components, formic acid,
87 acetic acid and methanol, are prebiotically plausible, and were likely abundant on early Earth
88 (McColom & Seewald, 2007; Mohammadi et al., 2020). Bicarbonate may support pyrite-
89 catalyzed carbon fixation, especially under high temperature and pressure (Cody et al., 2004).
90 Ammonium hydroxide and trimetaphosphate serve as sources of nitrogen and phosphorus
91 respectively.

92



93

94 **Figure 1.** Scheme of the experimental design.

95

96 **Experimental design.** We conducted chemical ecosystem selection involving a transfer-with-
97 dilution protocol (**Fig. 1**). First, we aliquoted 2 mL of FS with pyrite into glass vials (Neta
98 Scientific, RES-24658), sealed with rubber stoppers (Neta Scientific, W224100-400) and
99 aluminum seals (Neta Scientific, 224177-05). This procedure was conducted in an anaerobic
100 chamber (95% N₂, 5% H₂). The starting vials, designated generation 0, were autoclaved using a
101 liquid cycle (30 mins, 121°C, 30 psi) and incubated for 24 hours in a 40°C orbital shaking
102 incubator. Generation 1 vials received 1.6 mL FS and ~200 mg pyrite and either 0.4 mL (20%) of
103 the solution from a “parental” generation 0 vial or an additional 0.4 mL of fresh FS. Vials
104 receiving transfers (TRs) and no transfer controls (NTCs) were again autoclaved and incubated
105 for 24 hours. This procedure was repeated for 10 generations, with vials from each generation

106 stored at -80°C until analysis. In this work, our main analytical focus was to compare TRs to
107 NTCs every generation, as it allows us to control for experimental and analytical artifacts. We
108 conducted two identical replicate experiments, each with 10 TR lineages and 10 NTC pseudo-
109 lineages per generation. The results shown in this study are based on a combined analysis of
110 both experiments.

111 To help interpret the results and explain the role of pyrite and autoclaving in the
112 combinatorial explosion, we examined changes in chemical composition in FS over a single 24-
113 hour incubation period. FS solution was autoclaved and incubated or simply incubated with and
114 without pyrite, with samples taken every 2 hours. In addition to FS, we conducted a similar
115 procedure for samples that lacked subsets of FS components.

116

117 **Liquid-chromatography/mass-spectrometry (LCMS).** Immediately prior to chemical analysis,
118 vial contents were thawed and transferred to 96-well 0.2 mm filter plates (Neta Scientific, PALL-
119 8019) and vacuum filtered, to remove pyrite particles. We used an untargeted metabolomics
120 approach with reverse phase Ultra-Performance Liquid Chromatography coupled with tandem
121 mass-spectrometry (UPLC-MS/MS) with a Thermo Vanquish UPLC (Thermo Fisher Scientific,
122 Waltham, USA) with a C18 column (Agilent, Santa Clara, USA). Samples (5 μ L) were eluted in a
123 linear gradient mixture from 0.1% v/v formic acid in water (47146-M6, Thermo Fisher Scientific,
124 Waltham, USA) to 0.1% v/v formic acid in acetonitrile (47138-K7, Thermo Fisher Scientific,
125 Waltham, USA), over 14 min. To reduce the risk that order effects could yield artifactual
126 differences between TR and NTC treatments, samples were run with the first TR and NTC
127 replicates preceding the second replicate of each, and so on.

128 The UPLC was coupled to a Thermo Q-Exactive Plus Orbitrap MS (Thermo Fisher
129 Scientific, Waltham, USA). Full MS-SIM spectra for each of the replicates were collected for
130 10 minutes in positive mode over a scan range of 50–750 m/z, with resolution set to 70000.
131 Fragmentation data were collected only for pooled samples for each treatment category with
132 full MS followed by data-driven MS2 analysis (dynamic exclusion of 4s, intensity threshold
133 1.0E5, resolution 17500, isolation window 1 m/z, stepped collision energies of 20, 50 and 100
134 eV).

135

136 **Data structure.** Data in .raw format was processed in Compound Discoverer™ (Thermo Fisher
137 Scientific, Waltham, USA). We used a default untargeted metabolomics workflow with 16
138 added databases (Across Organics, Alfa Aesar, Alfa Chemistry, BioCyc, Cambridge Structural
139 Database, CAS Common Chemistry, ChemBank, DrugBank, FDA, Human Metabolome Database,
140 KEGG, MassBank, Merck Millipore, MeSH, NIST, NPAtlas) with pooled samples set to
141 'identification only'. Every sample from each experiment was processed in the same Compound
142 Discoverer analysis. Lists of identified compounds, their relative abundances and SMILES IDs
143 were extracted for downstream analyses. Additionally, for samples used to evaluate the role of
144 autoclaving and pyrite in generating chemical complexity, we ran samples individually in
145 Compound Discoverer™ in order to obtain comparable counts of the number of MS features.
146 Lists of identified compounds in the combined Compound Discoverer™ analysis, their relative
147 abundances and SMILES IDs were extracted for downstream analyses.

148 All features without assigned names or formulas were removed from the data due to
149 uncertainty about their identity and consequent difficulty in ensuring comparability between

150 samples. Areas of MS features were summed if they had the same name or, if names were
151 absent, the same formula. The resulting dataframes are lists of areas of identified compounds
152 in each sample and their assigned names/formulas.

153 To evaluate whether the TR and NTC samples in a generation are different, and whether
154 the degree of difference changes over generation, we calculated Canberra (**Eq. 1**) and Bray-
155 Curtis dissimilarities (**Eq. 2**) between each pair of samples using the vegan package in R
156 (Oksanen et al., 2007). These distance metrics are frequently used to quantify dissimilarity
157 between ecological communities (Ricotta & Podani, 2017). Since the Canberra distance sums
158 ratios rather than areas, it tends to weight each species more or less equally, regardless of its
159 absolute abundance, unlike Bray-Curtis which assigns higher weight to more abundant species.

$$d_{p,q} = \frac{1}{n} \sum_{i=1}^n \frac{|p_i - q_i|}{|p_i| + |q_i|}$$

160 **Equation 1.** Formula for Canberra distance: n – number of compounds; i – individual
161 compound; p – area of compound i in one sample; q – area of a compound i in a different
162 sample.

163

$$d_{p,q} = \frac{\sum_{i=1}^n |p_i - q_i|}{\sum_{i=1}^n (p_i + q_i)}$$

164
165 **Equation 2.** Formula for Bray-Curtis distance: n – number of compounds; i – individual
166 compound; p – area of compound i in one individual; q – area of a compound i in a different
167 individual.

168

169 To evaluate whether TR and NTCs differ, we compared the pairwise distances between
170 samples within groups (TRs and NTCs) with the between group distance (NTC-TR). We
171 conducted a permutational analysis of variance (PERMANOVA) in R. We calculated the mean
172 sum of square Canberra and Bray-Curtis distances and obtained standard deviations based on
173 500 bootstrap resamplings of features.

174

175 **Heritability calculations.** In evolutionary biology heritability is typically estimated as the slope
176 of a linear regression of trait values that have been measured in a set of parents and their
177 corresponding offspring. Since we have 20 parent/offspring pairs in each generation, we have
178 the capacity to calculate an analog of heritability for these data.

179 The first method we used is similar to the biological method and involves calculating the
180 Pearson correlation of the area of a compound in parents and offspring in adjacent generations
181 (e.g., generations 1 and 2, 2 and 3, etc.). We then compared the regression slope, r , over all
182 compounds to see if the null hypothesis of $r=0$ can be rejected using a t-test. We also calculated
183 the regression-based correlation for two summary statistics, namely the total number of
184 significantly enriched or depleted compounds relative to the set of NTCs from that generation.

185 To supplement the biological approach, we also developed a multivariate measure of
186 heritability, the Distance-base Heritability Index (DHI; **Eq. 3**). This index divides the distance

187 between parent-offspring pairs in adjacent generations with the mean distance between non-
188 parent-offspring pairs. Observing DHI values that are lower for TRs than NTCs would show that
189 samples from the same lineage are more similar to each other than would otherwise be
190 expected, thus supporting heritability. Our DHI calculations used the Canberra distance, which
191 weights all compounds equally, regardless of mean concentration.
192

$$DHI^{g,l} = \frac{CD_{g+1,l}^{g,l}}{\text{Average } CD_{g+1,l''}^{g,l'}}$$

193 **Equation 3.** Formula for the distance-based heritability index, DHI , as calculated for a parental
194 generation (g) relative to its offspring generation ($g + 1$). The average Canberra distance (CD) is
195 calculated between each vial in generation g and the corresponding vial from the same lineage
196 (l) in generation $g + 1$. This is then divided by the average distance calculated between each
197 parent vial and the offspring vials from all other (non-offspring) lineages (l' , l''). This metric is
198 calculated separately for lineages of TRs and pseudo-lineages of NTCs.
199

200 Finally, we applied a heredity metric developed by Guttenberg et al. (2015) for use in
201 studies of prebiotic chemistry. We used their Python script
202 (<https://github.com/ModelingOriginsofLife/Heredity/tree/master>) to analyze our data and
203 estimate the number of heritable states possible for the TRs, as compared to the NTCs. This
204 method conducts principal component analysis on an input set of properties for systems that
205 are inferred to have been exposed to different selective environments. The number of
206 eigenvalues above a computed threshold is taken as an estimate of the number of potentially
207 heritable states. This methodology can distinguish between intrinsic variation due to stochastic
208 processes and extrinsic variation due to selection based on the assumption that intrinsic
209 variation should be unimodal while extrinsic variation could be multimodal (Guttenberg et al.,
210 2015). We assumed that each generation experienced a somewhat different selective pressure
211 due to the differences in the amount of generation 0 material transferred into each vial.
212 Therefore, we estimated the number of heritable states per experimental lineage (N_s) with the
213 prediction of lower N_s in NTCs, which lack true intergenerational transmission. Prior to this
214 calculation, we normalized our dataset by subtracting the mean and dividing by the standard
215 deviation for each compound, as is a common practice for principal component analysis
216 (Guttenberg et al., 2015). The parameter alpha, which sets the sensitivity of the algorithm, was
217 set to 0.1.
218

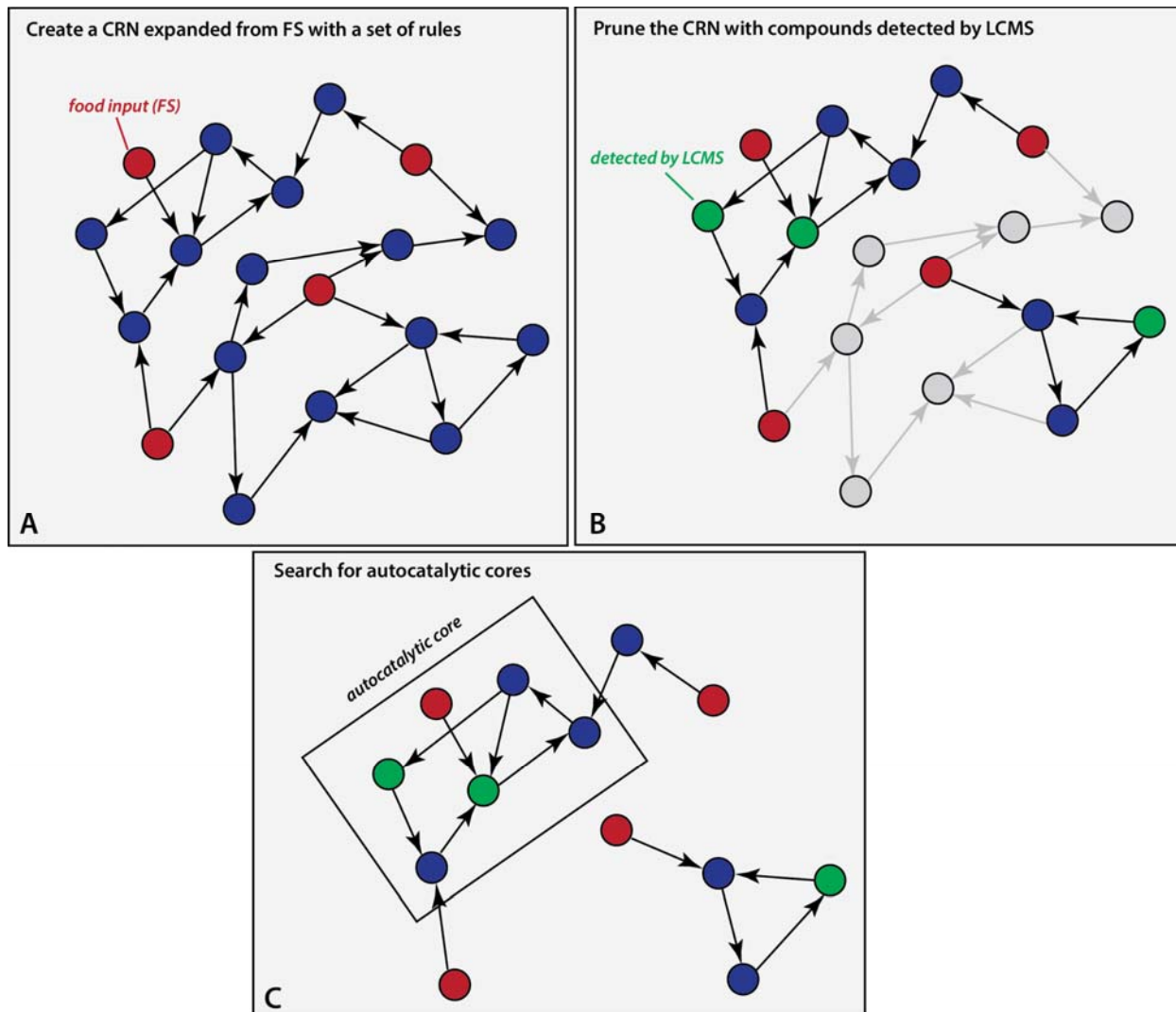
219 **Network expansion.** To explore the chemical pathways that could have generated the
220 compounds detected with LCMS from the initial FS we inferred a subset of the chemical
221 reactions that are likely occurring (Fig. 2) using a new rule-based chemical reaction generation
222 tool, Rule-It (Cuevas-Zuviria & Sokolskyi, 2024). Here, each round of network expansion uses
223 the compounds generated by all previous iterations and the initial food compounds to look for
224 new reactions that are allowable under a defined ruleset. To control the resulting combinatorial
225 explosion, the expansion algorithm in Rule-It allows for arbitrary or data-guided pruning, and

226 can be further constrained by molecular mass of the products (Cuevas-Zuviria & Sokolskyi,
227 2024).

228 Our ruleset included 16 reversible reaction types that could plausibly occur in our
229 samples, each written in SMARTS format (**Fig. C1, Tables C1-2**). This ruleset only included
230 reactions with oxygen, nitrogen, sulfur and phosphorus-containing functional groups. To
231 simplify analysis and reduce the total number of allowed reactions, we did not allow any ring-
232 forming reactions, although it is almost certain that some such reactions do occur in these
233 conditions. For computational simplicity, we also did not include rules that would generate the
234 well-known cyanide reaction network (Patel et al., 2015). For the initial set of compounds, we
235 include the six FS solutes plus water, sulfate, and hydrogen sulfide, the latter two being
236 plausible products of pyrite decomposition. Using a 40000 reaction limit and molecular weight
237 cap of 500, we ran four iterations of network expansion (**Fig. 2, A**).

238 To reduce the size of networks to a manageable size while focusing on potentially
239 relevant compounds, we pruned networks guided by experimental evidence. We identified all
240 compounds in the network that were detected by LCMS and pruned the network to include
241 these species and all reactions on the shortest reaction path to these compounds from the
242 initial set of compounds. All of the input files are available in Supplementary data.

243



244
245 **Figure 2.** Scheme of the computational pipeline for detecting autocatalytic cores (ACs): first, we
246 expand the network from the initial compound set (FS plus water, sulfate, and hydrogen
247 sulfide), shown in red, using our reaction ruleset (A); then we prune the resulting network
248 keeping only reactions and compounds (in blue) that lead from initial compound, to compounds
249 detected with LCMS (B); then we search for ACs in the pruned network (C).
250

251 **Detection of autocatalysis.** To detect autocatalytic cores (ACs), or minimal autocatalytic motifs,
252 in the pruned FS-driven CRN we utilized the program autocataytictsubnetworks (Gagrani et
253 al., 2024), which is downloadable from Github
254 (<https://github.com/vblancoOR/autocataytictsubnetworks>). Using that software, we
255 converted the pruned networks into stoichiometric matrices and then analyzed these to detect
256 stoichiometrically autocatalytic motifs (Fig. 2, C). To reduce computation time, we removed
257 rows representing water, carbon dioxide, ammonia and hydrogen sulfide from the input matrix,
258 thereby preventing us from detecting autocatalytic cores with these compounds as member
259 species. We did this because ACs with these ubiquitous compounds are poor candidates for
260 explaining heritability.

261

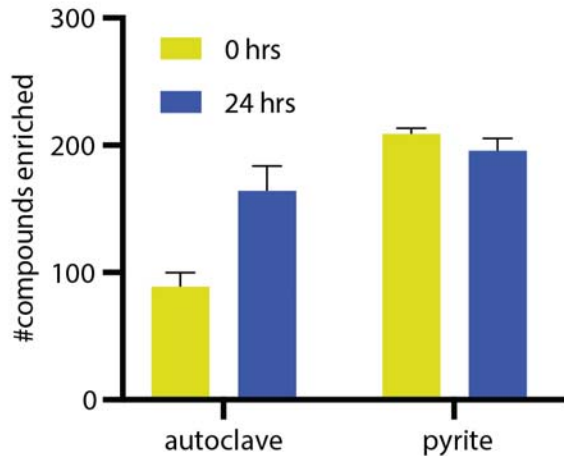
262

Results

263 **Pyrite and autoclaving promote chemical diversity.** To test for the existence of heritability, it
264 was necessary that the experimental system generated sufficient chemical complexity that
265 different lineages could, in principle, diverge from one another. Based on individual Compound
266 Discoverer™ runs we evaluated the average number of features above an arbitrary area
267 threshold of 10^6 for different treatments (**Supp. Table B1**). The largest factor seemed to be the
268 presence/absence of pyrite since more than 500 features were detected in samples with FS and
269 pyrite, compared to 166 without. The massive increase in the number of compounds seen after
270 incubation with pyrite with or without autoclaving can plausibly be explained by the chemistry
271 of the food as summarized in **Appendix A**. However, almost 500 features were also detected in
272 samples with water + pyrite, which might suggest that the effect of pyrite is partly due to
273 contamination. While we cannot rule this out, it is noteworthy that, almost all compounds
274 found in water + pyrite are undetected or at low abundance in FS + pyrite (**Fig. 3**). As result, it is
275 possible many represent analytical artifacts rather than contamination from pyrite. Sodium and
276 potassium salt clusters and other metal ions are a common electrospray ionization (ESI)
277 artifacts (McMillan et al., 2016), and likely correspond to many detected features, since FS
278 includes two sodium salts (bicarbonate and trimetaphosphate). Differences in pyrite oxidation
279 between water and FS could also affect feature counts as Fe adducts are known to be another
280 ESI artifact (Bonner & Hopfgartner, 2022). Hence it is unclear whether absolute feature counts
281 accurately represent chemical diversity of our samples.

282 Combined analysis in CompoundDiscoverer™ makes it possible to directly compare the
283 mass spectral features between samples, at the cost that all compounds that are detected in
284 any sample are assigned an imputed area in all other samples, whether or not they were
285 detected. To get around this problem and quantitatively assess how pyrite and autoclaving
286 affect compound abundances, we counted up the number of compounds that have significantly
287 elevated areas in one treatment relative to another (**Fig. 3**). The effect of autoclaving was
288 assessed by comparing FS without pyrite to autoclaved FS over the course of a 24 hour
289 incubation. The effect of pyrite was determined by comparing unautoclaved FS with pyrite to
290 unautoclaved FS without pyrite. These analyses revealed that an “explosion” of chemical
291 diversity occurred both due to either autoclaving or pyrite addition, with pyrite having a greater
292 and more immediate effect.

293



294
295

296 **Figure 3.** Number of detected compounds with area $>10^6$ significantly enriched relative to
297 respective controls ($>2 \times \text{SD}$ difference: compared to unautoclaved samples without pyrite for
298 autoclave effect; compared to unautoclaved samples without pyrite and to water with pyrite
299 for pyrite effect) in FS due to autoclaving or pyrite. Error bars are SEM.

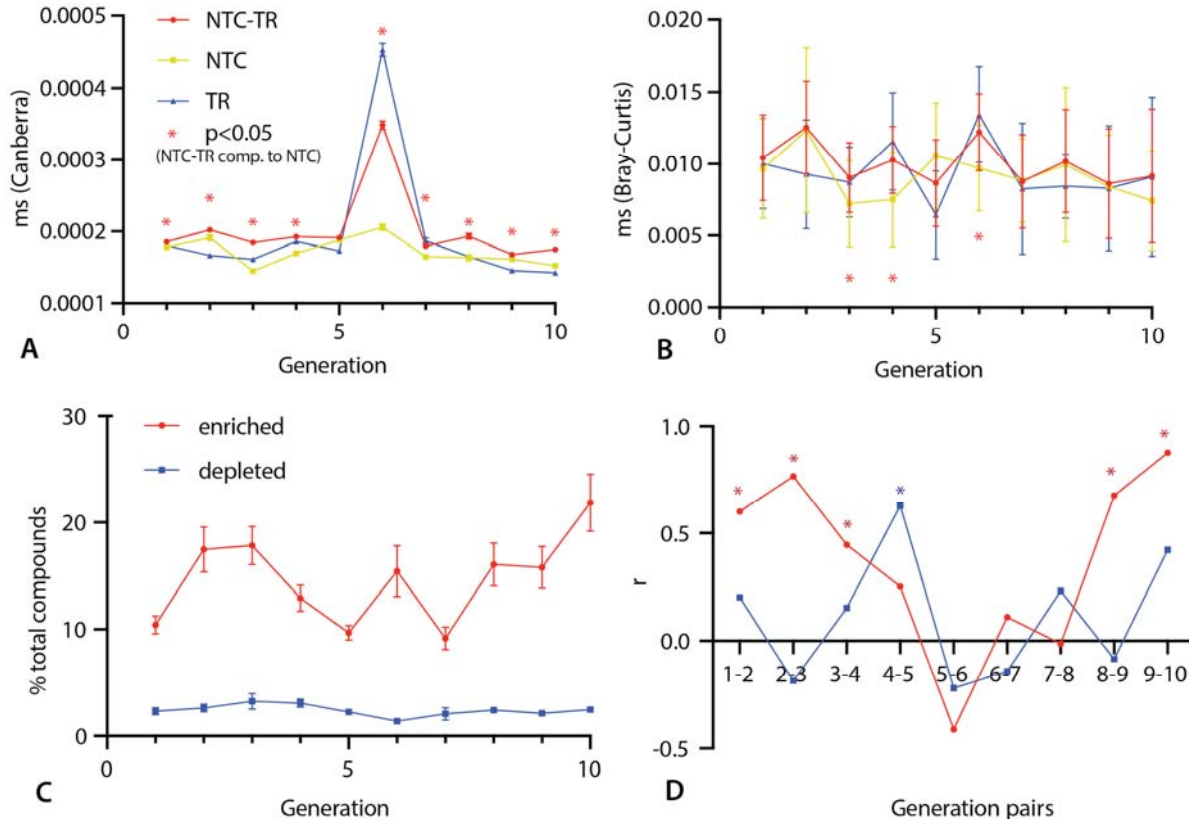
300

301 **Transfer samples diverge from controls.** To quantify the divergence between transfer lineages
302 and control lineage, we conducted PERMANOVA analysis on Canberra and Bray-Curtis
303 distances. For Canberra distances NTC-TR distances are greater than either NTC-NTC or TR-TR
304 distances, except for generation 6 when TR-TR distances are higher. This difference was
305 significant ($p < 0.05$) in every generation except generation 5 (Fig. 4, A). Bray-Curtis distances
306 also tend to be more similar within than between groups, but NTC-TR and NTC-NTC are
307 significantly different only in generations 3, 4 and 6 (Fig. 4, B). Taken together, the tendency for
308 greater NTC-TR distances than within-group distances shows that the presence of material
309 transferred from prior generations significantly affects the overall composition of vials.

310 In addition to distance metrics, we also calculated the number of compounds that are
311 significantly ($>2 \times \text{SD}_{\text{NTC}}$ difference) enriched and depleted in TRs compared to NTCs within a
312 generation (Fig. 4, C). Since TRs carry forward products from one generation to the next, we
313 predicted that there would often be compounds that are only seen above the threshold of
314 detection in TRs. Indeed, about ten times as many compounds are enriched than depleted
315 when comparing TRs and NTCs. While the number of depleted compounds remains similar
316 across all 10 generations, the fraction of compounds that are significantly enriched in TRs varies
317 markedly across generations (9-22%).

318 We calculated the Pearson correlation coefficients between the number of enriched and
319 depleted compounds in parent-offspring pairs (Fig. 4, D). While the slope of the regression of
320 depleted compounds fluctuates, there is generally a positive correlation for enriched
321 compounds, meaning that parent vials with a higher or lower count of enriched compounds
322 tend to give rise to offspring vials that also have a higher or lower number, respectively. This
323 parent-offspring correlation has a significant slope ($p < 0.05$), suggesting heritability, for five
324 generation pairs, the first three and the last two (Fig. 4, D).

325



326
327 **Fig. 4.** Dynamic changes over the course of the experiment. **A** – mean sum of squares (ms) of
328 inter-group Canberra distance, plotted are TR-NTC, NTC-NTC and TR-TR group distances; **B** –
329 mean of squares (ms) of inter-group Bray-Curtis distance, plotted are TR-NTC, NTC-NTC and TR-
330 TR group distances; **C** – change in the number of compounds significantly (difference greater
331 than $2 \times \text{SD}_{\text{NTC}}$) enriched or depleted in TRs compared to NTCs every generation; **D** – Pearson
332 correlation of the number of enriched and depleted compounds between adjacent generations
333 in the TR treatment (significant correlation, $p < 0.05$, is marked by asterisks). Error bars are SD in
334 A-B and SEM in C.

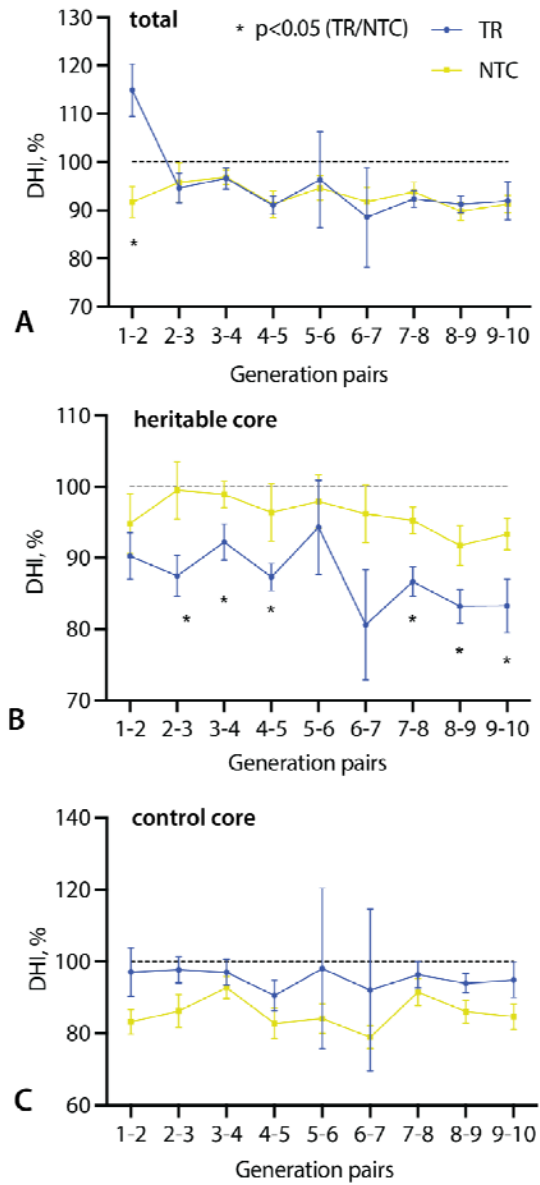
335
336 **Heritability of chemical composition.** More individual compounds have significantly positive
337 parent-offspring correlations than expected by chance, but a similar fraction was seen in both
338 TRs and NTCs despite the fact that NTCs have no true “parent-offspring” relationships. Similarly,
339 although average regression slopes are significantly greater than 0 in many generations, these
340 were found in both TRs and NTCs with no clear pattern (Fig. B1). The most likely explanation of
341 these results is not heritability but the order in which samples were analyzed in LC-MS. Lower-
342 numbered replicates of both NTCs and TRs tended to be loaded earlier in an LC-MS run than
343 high-numbered replicates, which can yield a false signal of heritability when column properties
344 or MS sensitivity changes over time.

345 In order to obtain a single metric that summarizes all data, we developed the DHI
346 statistic, which measures whether parent-offspring pairs are more similar than unrelated vials
347 from their respective generations. When calculating DHI using the Canberra distance matrix for
348 the complete, filtered dataset we observed no difference between TR and NTC values, which

349 are all in 90-100% range, except for generation 1, where the DHI of TRs is significantly ($p<0.05$)
350 greater than in NTCs (**Fig. 5, A**).

351 Given the possibility that a strong order-of-analysis effect might be swamping true
352 signals of heritability we recalculated DHI based only on compounds that are the strong
353 candidates for being heritable in TRs but not NTCs and, as a control, those that are candidates
354 for showing higher “heritability” in NTCs. To be a candidate in either direction, a compound
355 showed Pearson correlation coefficients greater than 0.5 in 3 or more pairs of generations for
356 one of the data sets (TR or NTC), but for 1 or fewer pairs of generations for the other data set.
357 Recalculating DHI for the heritable candidate sets yielded different results for TR and NTC data
358 (**Fig. 5, B-C**). In both cases the DHI for the candidates is reduced as expected if there were
359 heritability. This could be due, in part, to selecting those compounds that had a pattern of
360 apparent heritability. However, the DHI decline was much greater when the compounds were
361 selected based on apparent heritability in the TRs (**Fig. 5B**) than for the NTCs (**Fig. 5C**).
362 Statistical tests never detected a significant difference in DHI between NTCs and TRs for the
363 NTC candidates, but the TR DHI is significantly lower than those for NTCs in 6 out of 9
364 generation pairs for the TR heritable core (**Fig. 5, B-C**).
365

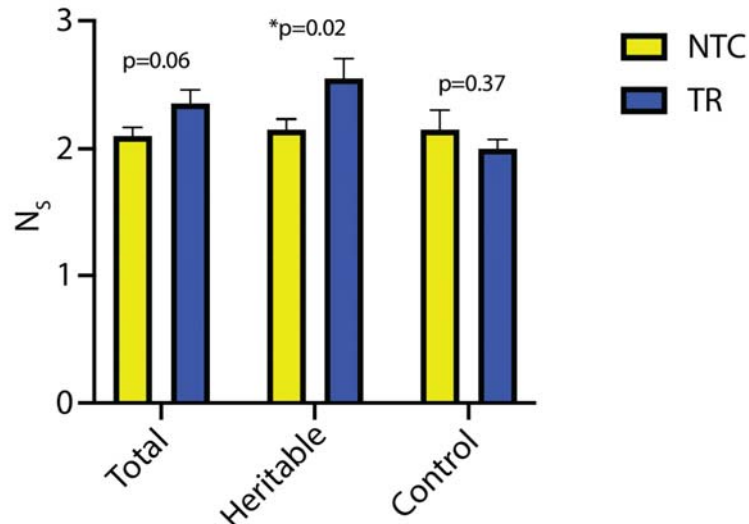
366 We also estimated the number of possible heritable states for the full dataset and the
367 two candidate subsets, using the method of Guttenberg et al. (2015). For the total dataset we
368 find that TR lineages have more possible heritable states with a close to significant p-value of
369 0.06 (**Fig. 6**). For the TR candidates the difference is even more significant ($p = 0.02$), while for
370 the NTC candidate no significant difference was detected ($p=0.37$).



371

372

373 **Fig. 5.** Changes in heritability as measured by the distance-based heritability index (DHI) using
374 Canberra distance matrix. **A** – change in DHI over the course of the experiment for the whole
375 compound dataset; **B** – change in DHI for the dataset comprising the “heritable core” –
376 compounds that have $r > 0.5$ in 3 or more pairs of generations of TRs, and 1 or less generations
377 of NTCs; **C** – change in DHI for the control dataset – compounds that have $r > 0.5$ in 1 or less pairs
378 of generations of TRs, and 3 or more generations of NTCs. Error bars are SEM.



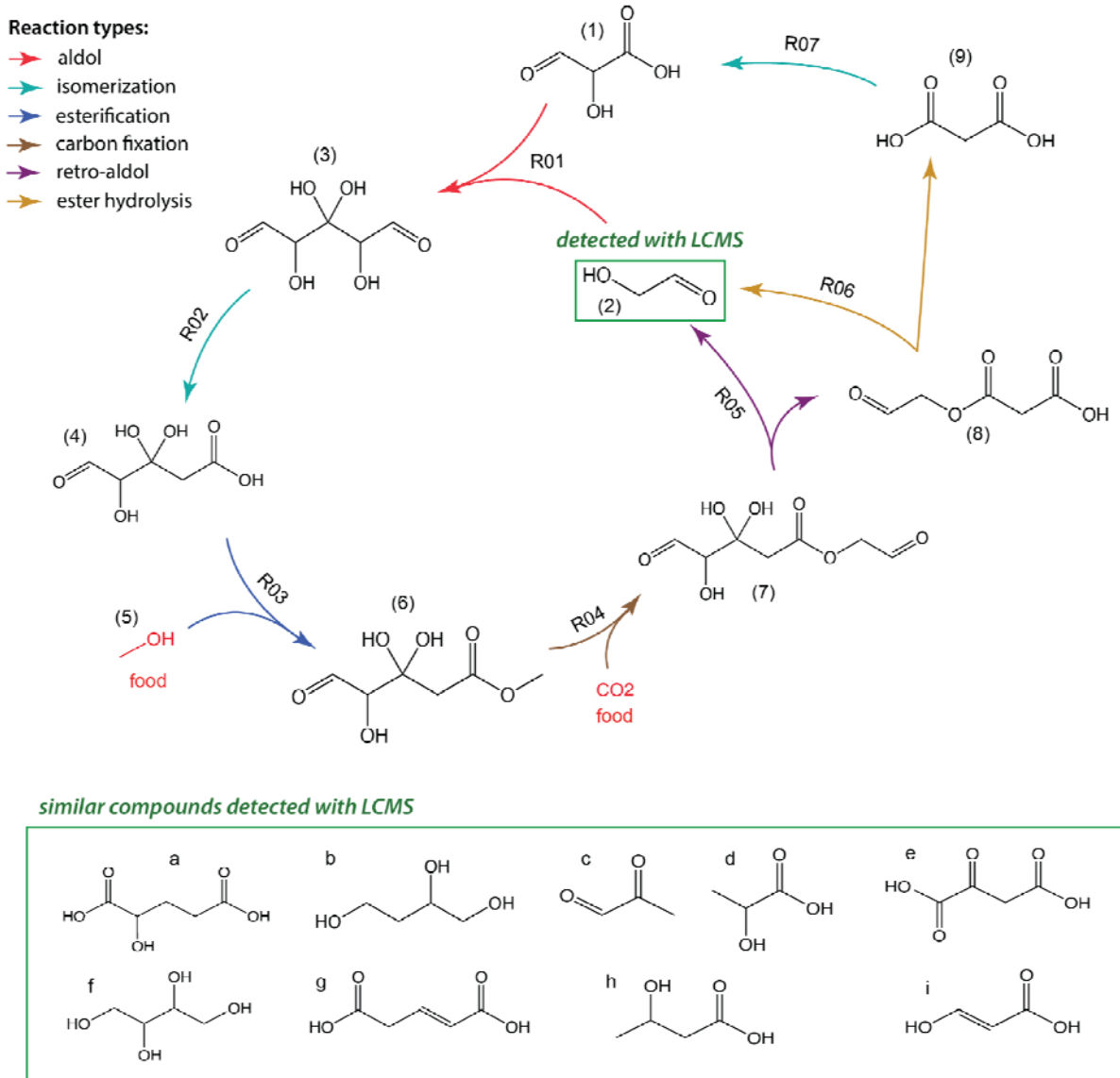
379
380 **Fig. 6.** Number of heritable states (N_s), for the total dataset, heritable core (only compounds
381 with $r>0.05$ for >3 pairs of generations of TRs and <1 of NTCs) and control core (only
382 compounds with $r>0.05$ for >3 pairs of generations of NTCs and <1 of TRs). Error bars are SEM.
383

384 **CRN reconstruction and analysis.** Using the FS as the input and the ruleset shown in Table C2,
385 one round of expansion yielded a CRN of 22 reactions and 28 compounds (Fig. C2). This
386 increased to 332 reactions and 282 compounds after two rounds, 7869 reactions and 6719
387 compounds after three, and 40395 reactions and 33873 compounds after 4. In the latter CRN,
388 47 compounds could be matched to features that were detected and identified by LCMS. Of the
389 6 (1.5%) or the 412 compounds that were candidates for heritability based on the NTCs and 3
390 (1.9%) of the 160 compounds in the TR candidates were included in the network. Such low
391 numbers are expected, as our ruleset likely represents a small fraction of possible FS-driven
392 reactions. The numbers of reactions for each rule are summarized in supplementary Fig. C3.

393 In the resulting CRNs pruned on either all 47 detected compounds or the two candidate
394 sets, we detected multiple autocatalytic cores (ACs), each including from 10 to 34 reactions.
395 There were 419 ACs for the network pruned with all LCMS hits, 1 for the NTC heritable
396 candidates, and 14 for the TR heritable candidates. Many of the ACs included nitrogen- or
397 sulfur- containing compounds, some included only carbon, oxygen, and hydrogen. An example
398 of the latter is shown in Fig. 7. We were unable to detect any ACs in the pruned network whose
399 food consisted only of compounds in the FS, meaning that at least one food has to be produced
400 by other reactions that are not part of the AC. However, for many of the ACs the food
401 compounds are relatively simple, e.g., formic acid, small imines, or methanol. Additionally,
402 because some key reactions are removed during network pruning, there are likely additional
403 pathways for generating some food species. For example, R07 in Fig. 7 was not present in the
404 pruned network - and thus the AC had species (1) as a food and species (9) as a waste species.
405 However, R07 was present in the full network resulting from network expansion.

406 For none of the detected ACs were all of the member species detected and identified by
407 LCMS. This could of course be due to analytical constraints, but could also be the result of
408 certain member species having low equilibrium concentrations, for example due to them being

409 unstable intermediates. However, in many cases chemically similar species were detected. For
410 the AC in **Fig. 7** only glycolaldehyde (2) was detected but there are multiple alcohols, aldehydes
411 and carboxylic acids in the LCMS data similar to other AC member species. For example,
412 compound d (lactic acid) only differs from compound 1 (2-hydroxy-3-oxopropanoic acid) by one
413 carbonyl group.
414



415
416
417 **Figure 7.** An example AC detected in the CRN pruned with heritable candidates from the TR.
418
419 **Discussion**
420 **Autoclaving, pyrite and transfers significantly impact chemical diversity.** Both autoclaving and
421 pyrite result in the appearance of many more compounds in FS (Fig. 3). Pyrite had the greatest
422 effect, presumably because of the ability of pyrite and other metal-rich minerals to catalyze

423 prebiotically-relevant reactions, including abiotic carbon fixation, incorporation of nitrogen into
424 organic compounds, and the formation of larger organics (de Graaf et al, 2023; Asche et al.,
425 2024). Carbon fixation with CO₂, or similar reactions starting with 1 and 2 carbon organic
426 molecules, seem particularly relevant and necessary to explain the many larger organic
427 compounds we detected after incubation. As outlined in Appendix A, we can draw on changes
428 in vial composition over the course of a 24-hour incubation to speculate as to a few chemical
429 reactions that might be occurring during incubation with pyrite.

430 In order to have any possibility of revealing heritability, it is first essential that the
431 transfer process affects the chemical composition of TR vials relative to NTC vials, which receive
432 no inputs from the prior generation. Indeed, we find clear evidence of systematic differences
433 between TR and NTC vials in almost all generations, as shown by greater average TR-NTC
434 Canberra distances than either TR-TR or NTC-NTC (Fig. 4, A). The fact that this effect is less clear
435 using Bray-Curtis distances (Fig. 4, B) likely reflects the fact that this distance measure tends to
436 be dominated by a few high-abundance compounds.

437

438 **Heritability can be detected in small-molecule chemical systems.** In this study we used
439 multiple parallel parent-offspring transfer lineages to detect heritable variation emerging from
440 prebiotically plausible reactions. Here we understand heritability, analogously to biology, as the
441 fraction of the variation between individuals in a population that is inherited from parents to
442 offspring (Visscher et al., 2008). In this context, the 20 TR vials in adjacent generations comprise
443 the population of parents and offspring and the phenotypes are areas of different mass-
444 spectral features.

445 To be relevant to long term evolution, heritable differences among vials would need to
446 be the result of autocatalytic cycles that are activated in some but not all vials. However, any
447 given autocatalytic cycle may have only a small number of detectable members meaning that
448 only a tiny fraction of compounds will show heritability, with the remaining variation being due
449 to experimental noise. Thus, the fact that we did not find many compounds in TR vials that had
450 high parent-offspring correlations is insufficient to reject the hypothesis of heritability.

451 Three analyses supported the idea that heritability is present in this system. First, a
452 system-level, emergent trait, the number of enriched compounds, shows a pattern consistent
453 with heritability (Fig. 4, D). Second, we found DHI to be significantly higher for the TR heritable
454 candidates in most generations, whereas no such pattern is seen using the NTC candidates (Fig.
455 5). Third, the number of heritable states in TRs tends to be significantly greater than in NTCs
456 (Fig. 6). The latter is more a metric of evolvability than heritability, and may be sensitive to the
457 larger number of enriched compounds in TRs than NTCs, but seems to confirm the general
458 pattern that transfer lineages have the potential to diverge from one another over time.
459 Collectively, these analyses provide the first direct evidence that chemical systems driven from
460 equilibrium by prebiotically plausible chemical food sets can vary and pass on those variations
461 into the future. This is important because the generation of heritable variation is a minimal
462 requirement for evolution by natural selection.

463 To evaluate the significance of this result, it is worth considering whether these patterns
464 could arise by trivial mechanisms, of which the most obvious is contaminants being introduced
465 into a subset of parent vials that are then seen at elevated concentrations in offspring vials
466 simply because the latter receive, as input, 20% of the volume from their parent vial. If such

467 contaminants did not react, we would expect them to occur at five-fold lower concentration in
468 offspring than parents. A positive correlation between parents and offspring could be seen,
469 nonetheless, but only if the magnitude of the contamination received by parents is five times
470 greater than the threshold of detection by LC-MS. We believe that such high-concentration
471 contaminants are likely rare, so we take the evidence of heritability as suggestive of
472 autocatalysis.

473 **Autocatalysis and heritability.** Our hypothesis is that variation in parent vials arises from time
474 to time, whether from sub-threshold contamination or stochastic chemical dynamics, and this
475 triggers novel autocatalytic processes that are passed onto offspring vials. Consistent with this,
476 we detected multiple stoichiometric ACs in the partial CRN that we inferred using a limited
477 number of reaction rules, while disallowing cyclization reactions. Moreover, even with these
478 constraints, the number of ACs detected was surely a large underestimate. First, due to the
479 probabilistic nature of the expansion algorithm, some important reactions would have been
480 missed. This is illustrated by R07 in Fig. 7, which was present in the unpruned network, but was
481 removed after pruning. Second, Rule-it only considers uncatalyzed unit reactions, disallowing
482 cases of catalysis, where the same compound appears both as a reactant and product. Third,
483 we were forced to limit the network expansion to just four iterations due to computational
484 constraints, whereas the number of autocatalytic motifs tends to scale exponentially with CRN
485 size (Mossel and Steel, 2005; Gagrani et al. 2024). These factors suggest that the number of ACs
486 we detected is a significant undercount.

487 A promising finding that could be taken as supporting our inference, is that the CRN
488 pruned based on the 3 members of the heritable core set contained 14 ACs, as contrasted with
489 just one in the network pruned based on the NTC candidate set. If heritability is associated with
490 autocatalysis, we expected the TR heritable candidates to include members ACs - while AC
491 members in the NTC candidates must be random. However, we must be cautious about this
492 observation, as it could easily be a stochastic artifact due to the small number of compounds
493 detected in each case.

494 To support heritability, it is not sufficient that stoichiometric ACs be present, they also
495 would need to be kinetically viable (Steel et al., 2019). For example, a food species for an AC
496 may not be produced at a sufficient rate to allow for exponential growth of member species or
497 side reactions may consume some member species at rates greater than the AC reactions
498 (Orgel, 2008). Thus, it would be desirable to obtain data on plausible rate constants of different
499 reactions or, better still, to experimentally validate inferred ACs.

500 Even if kinetically viable, an AC could only support heritability if it differed in flux
501 between lineages, the extreme being the case where it is active only in a subset of vials that
502 were seeded by slow reactions or occasional contamination (Peng et al., 2022). Whether or not
503 this can be experimentally shown, it highlights the potential importance of rare events and
504 chemical diversity in prebiotic evolution, which contrasts with the focus on high-yield reactions
505 that lead to particular target molecules, which has dominated much prior research in prebiotic
506 chemistry.

507 This work provides the first statistical evidence for the spontaneous emergence of
508 heritable variation in prebiotically plausible chemical mixtures. Additionally, we developed a
509 novel set of methods for quantifying heritability and connecting it with the underlying chemical
510 reaction network. This represents a significant advance towards the goal of understanding how

511 systems capable of adaptive evolution could have bootstrapped themselves into existence on
512 the early Earth. Moreover, while there are areas where the protocol could be improved, most
513 obviously by randomizing LC-MS analysis order to remove order-of-analysis effects, our
514 experimental approach and the metrics developed may serve as a blueprint for further
515 investigations into the emergence of heritability and evolvability in the absence of genetic
516 polymers.

517

518 **Acknowledgments.** The authors would like to thank Zoe Todd, John Yin, Betül Kaçar, Daniel
519 Amador-Noguez and Annie Bauer for feedback on this project. We would like to thank Chris
520 Thomas, Julia Duncan and Eric Armstrong for valuable guidance on LCMS operation and data
521 analysis. We would like to thank Praful Gagrani for clarifications on mathematical concepts and
522 Lena Vincent for help with experimental design. We thank Cécile Ané from the Statistical
523 Consulting group at the University of Wisconsin – Madison for assistance in the analysis of the
524 experiment. This research was funded by the Department of Botany at the University of
525 Wisconsin–Madison and the National Science Foundation (grant number DEB 2218817).

526

527 **Conflicts of interest.** None declared.

References

528

529

530 Arya, A., Ray, J., Sharma, S., Simbron, R.C., Lozano, A., Smith, H.B., Andersen, J.L., Chen, H.,
531 Meringer, M. and Cleaves, H.J. (2022). An open source computational workflow for the
532 discovery of autocatalytic networks in abiotic reactions. *Chemical Science*, 13(17),
533 pp.4838-4853.

534 Asche, S., Pow, R. W., Mehr, H. M., Cooper, G. J., Sharma, A., & Cronin, L. (2024). Evidence of
535 Selection in Mineral Mediated Polymerization Reactions Executed in a Robotic
536 Chemputer System. *ChemSystemsChem*, 6(3), e202400006.

537 Baum, D. A., & Vetsigian, K. (2017). An experimental framework for generating evolvable
538 chemical systems in the laboratory. *Origins of Life and Evolution of Biospheres*, 47, 481-
539 497.

540 Baum, D. A. (2018). The origin and early evolution of life in chemical composition space. *Journal*
541 *of theoretical biology*, 456, 295-304.

542 Baum, D. A., Peng, Z., Dolson, E., Smith, E., Plum, A. M., & Gagrani, P. (2023). The ecology–
543 evolution continuum and the origin of life. *Journal of the Royal Society*
544 *Interface*, 20(208), 20230346.

545 Bonner, R., & Hopfgartner, G. (2022). Annotation of complex mass spectra by multi-layered
546 analysis. *Analytica Chimica Acta*, 1193, 339317.

547 Cody, G. D., Boctor, N. Z., Brandes, J. E. A., Filley, T. R., Hazen, R. M., & Yoder Jr, H. S. (2004).
548 Assaying the catalytic potential of transition metal sulfides for abiotic carbon
549 fixation. *Geochimica et Cosmochimica Acta*, 68(10), 2185-2196.

550 Colón-Santos, S., Cooper, G. J., & Cronin, L. (2019). Taming the combinatorial explosion of the
551 formose reaction via recursion within mineral environments. *ChemSystemsChem*, 1(3),
552 e1900014.

553 Cuevas-Zuviria, B. & Sokolskyi, T. (2024). Rule-it: an online platform for chemical reaction
554 network explorations for chemical evolution. *chemrxiv*, doi: 10.26434/chemrxiv-2024-
555 nqwpb

556 de Graaf, R., De Decker, Y., Sojo, V., & Hudson, R. (2023). Quantifying Catalysis at the Origin of
557 Life. *Chemistry—A European Journal*, 29(53), e202301447.

558 Gagrani, P., Blanco, V., Smith, E., & Baum, D. (2024). Polyhedral geometry and combinatorics of
559 an autocatalytic ecosystem. *Journal of Mathematical Chemistry*, 62(5), 1012-1078.

560 Guttenberg, N., Laneuville, M., Ilardo, M., & Aubert-Kato, N. (2015). Transferable
561 measurements of Heredity in models of the Origins of Life. *PLoS one*, 10(10), e0140663.

562 Guttenberg, N., Virgo, N., Chandru, K., Scharf, C., & Mamajanov, I. (2017). Bulk measurements
563 of messy chemistries are needed for a theory of the origins of life. *Philosophical
564 Transactions of the Royal Society A: Mathematical, Physical and Engineering
565 Sciences*, 375(2109), 20160347.

566 Happel, R., & Stadler, P. F. (1999). Autocatalytic replication in a CSTR and constant
567 organization. *Journal of mathematical biology*, 38(5), 422-434.

568 Joyce, G. F. (1994). Forward. *Origins of Life: The Central Concepts*. W. Deamer and GR
569 Fleischaker, eds.

570 Lu, H., Blokhuis, A., Turk-MacLeod, R., Karuppusamy, J., Franconi, A., Woronoff, G., ... &
571 Griffiths, A. D. (2024). Small-molecule autocatalysis drives compartment growth,
572 competition and reproduction. *Nature Chemistry*, 16(1), 70-78.

573 Lush, J. L. (1937) *Animal Breeding Plans*. Ames, Iowa: Iowa State Press.

574 Matange, K., Rajaei, V., Capera-Aragonès, P., Costner, J. T., Robertson, A., Kim, J. S., ... & Pinter,
575 M. F. (2023). Evolution of complex chemical mixtures reveals combinatorial compression
576 and population synchronicity.

577 McCollom, T. M., & Seewald, J. S. (2007). Abiotic synthesis of organic compounds in deep-sea
578 hydrothermal environments. *Chemical reviews*, 107(2), 382-401.

579 McMillan, A., Renaud, J. B., Gloor, G. B., Reid, G., & Sumarah, M. W. (2016). Post-acquisition
580 filtering of salt cluster artefacts for LC-MS based human metabolomic studies. *Journal of
581 cheminformatics*, 8, 1-5.

582 Mohammadi, E., Petera, L., Saeidfirozeh, H., Knížek, A., Kubelík, P., Dudžák, R., Krůš, M., Juha, L.,
583 Civiš, S., Coulon, R. and Malina, O., 2020. Formic acid, a ubiquitous but overlooked
584 component of the early earth atmosphere. *Chemistry—A European Journal*, 26(52),
585 pp.12075-12080.

586 Oksanen, J., Kindt, R., Legendre, P., O'Hara, B., Stevens, M. H. H., Oksanen, M. J., & Suggests, M.
587 A. S. S. (2007). The vegan package. *Community ecology package*, 10(631-637), 719.

588 Patel, B. H., Percivalle, C., Ritson, D. J., Duffy, C. D., & Sutherland, J. D. (2015). Common origins
589 of RNA, protein and lipid precursors in a cyanosulfidic protometabolism. *Nature
590 chemistry*, 7(4), 301-307.

591 Paul, N., & Joyce, G. F. (2004). Minimal self-replicating systems. *Current opinion in chemical
592 biology*, 8(6), 634-639.

593 Peng, Z., Kaçar, B., Fahrenbach, A., & Adam, Z. (2023). An assessment of stoichiometric
594 autocatalysis across element groups. *chemrxiv*

595 Peng, Z., Linderoth, J., & Baum, D. A. (2022). The hierarchical organization of autocatalytic
596 reaction networks and its relevance to the origin of life. *PLOS Computational
597 Biology*, 18(9), e1010498.

598 Peng, Z., Plum, A. M., Gagrani, P., & Baum, D. A. (2020). An ecological framework for the
599 analysis of prebiotic chemical reaction networks. *Journal of theoretical biology*, 507,
600 110451.

601 Ricotta, C., & Podani, J. (2017). On some properties of the Bray-Curtis dissimilarity and their
602 ecological meaning. *Ecological Complexity*, 31, 201-205.

603 Roszak, R., Wołos, A., Benke, M., Gleń, Ł., Konka, J., Jensen, P., Burgchardt, P., Żądło-
604 Dobrowolska, A., Janiuk, P., Szymkuć, S. and Grzybowski, B.A. (2024). Emergence of
605 metabolic-like cycles in blockchain-orchestrated reaction networks. *Chem*, 10(3),
606 pp.952-970.

607 Segré, D., Ben-Eli, D., Deamer, D. W., & Lancet, D. (2001a). The lipid world. *Origins of Life and
608 Evolution of the Biosphere*, 31, 119-145.

609 Segré, D., Shenhav, B., Kafri, R., & Lancet, D. (2001b). The molecular roots of compositional
610 inheritance. *Journal of Theoretical Biology*, 213(3), 481-491.

611 Sokolskyi, T., Ganju, P., Montgomery-Taylor, R., & Baum, D. A. (2024). Evidence of Heritability in
612 Prebiotically Realistic Membrane-Bound Systems. *Life*, 14(3), 284.

613 Srivastava, R., Dueñas-Díez, M., & Pérez-Mercader, J. (2018). Feed rate noise modulates
614 autocatalysis and shapes the oscillations of the Belousov–Zhabotinsky reaction in a
615 continuous stirred tank reactor. *Reaction Chemistry & Engineering*, 3(2), 216-226.

616 Steel, M., Hordijk, W., & Xavier, J. C. (2019). Autocatalytic networks in biology: structural theory
617 and algorithms. *Journal of the Royal Society Interface*, 16(151), 20180808.

618 Vasas, V., Fernando, C., Santos, M., Kauffman, S., & Szathmáry, E. (2012). Evolution before
619 genes. *Biology direct*, 7, 1-14.

620 Vasas, V., Fernando, C., Szilágyi, A., Zachár, I., Santos, M., & Szathmáry, E. (2015). Primordial
621 evolvability: Impasses and challenges. *Journal of theoretical biology*, 381, 29-38.

622 Vasas, V., Szathmáry, E., & Santos, M. (2010). Lack of evolvability in self-sustaining autocatalytic
623 networks constraints metabolism-first scenarios for the origin of life. *Proceedings of the
624 National Academy of Sciences*, 107(4), 1470-1475.

625 Visscher, P. M., Hill, W. G., & Wray, N. R. (2008). Heritability in the genomics era—concepts and
626 misconceptions. *Nature reviews genetics*, 9(4), 255-266.

627 Wächtershäuser, G. (1988). Pyrite formation, the first energy source for life: a
628 hypothesis. *Systematic and Applied Microbiology*, 10(3), 207-210.

629 Warr, W. A. (1997). Combinatorial chemistry and molecular diversity. An overview. *Journal of
630 chemical information and computer sciences*, 37(1), 134-140.

631 Wołos, A., Roszak, R., Żądło-Dobrowolska, A., Beker, W., Mikulak-Klucznik, B., Spólnik, G., ... &
632 Grzybowski, B. A. (2020). Synthetic connectivity, emergence, and self-regeneration in
633 the network of prebiotic chemistry. *Science*, 369(6511), eaaw1955.